# Supplemental Figure 1.

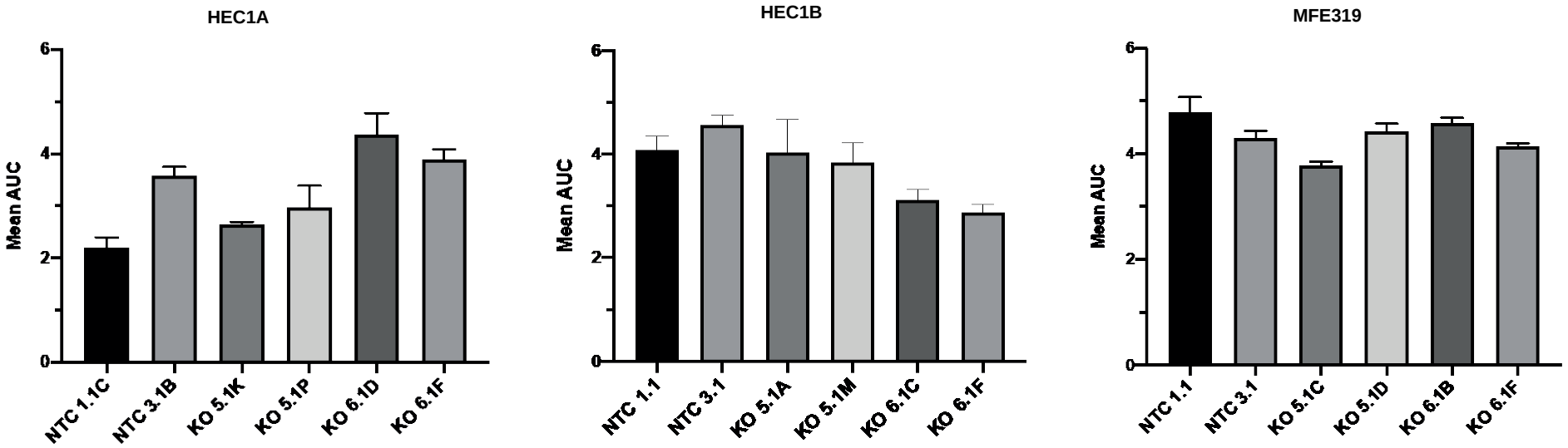


TP53 knockout via CRISPR/Cas9 in three EC cell lines with GOF/DN alleles and high VAF (presumed loss-of-heterozygosity) does not impact radiation response.

# Supplemental Figure 2.

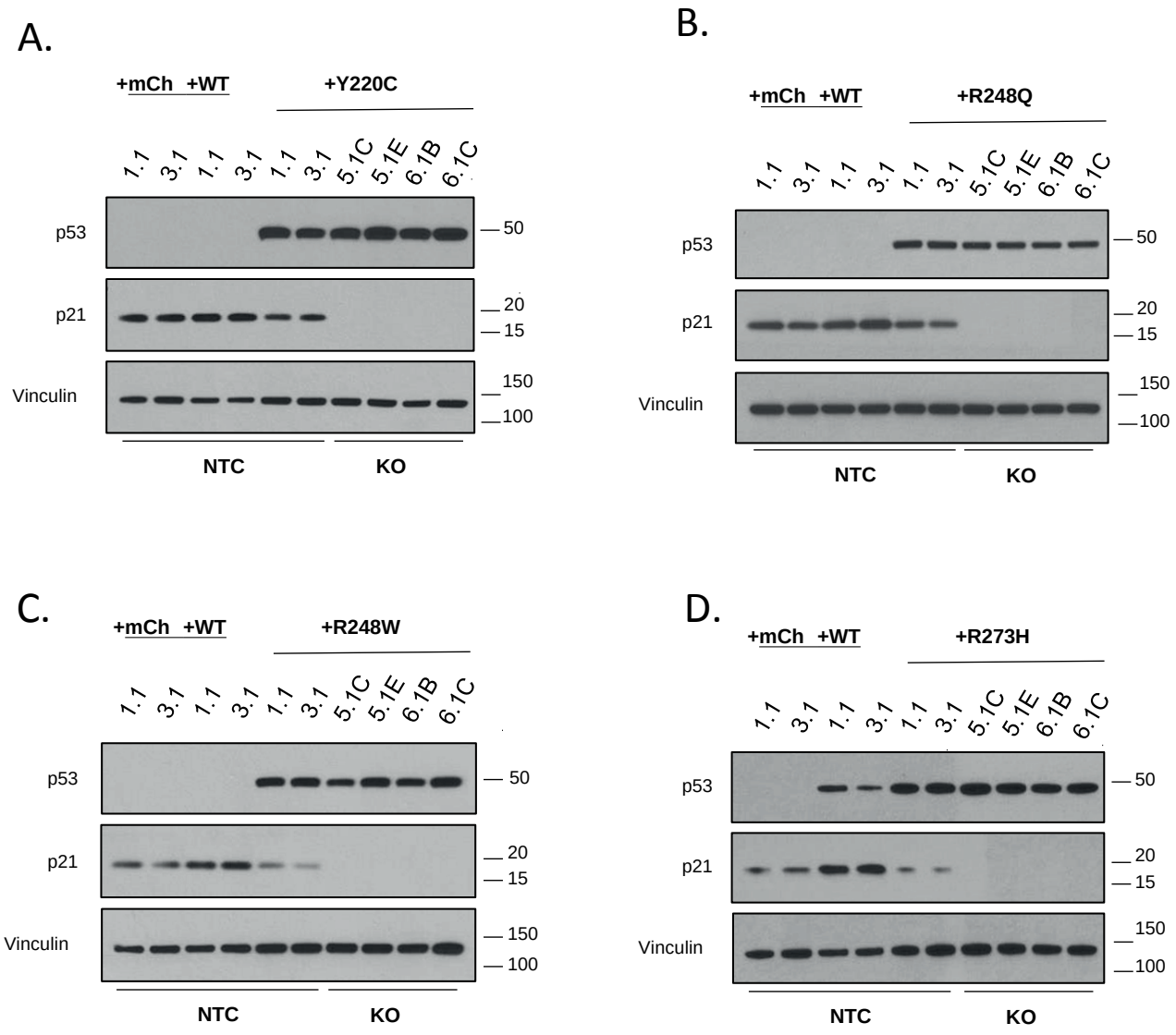


Western-blot analysis of 4 alternative TP53 alleles reveal abrogation of p21 signaling by the mutant allele in the presence of two wild-type alleles. As seen in the knock-out monoclonal lines (5.1C/E and 6.1B/C) expression of the mutant allele alone does not impact p21 signaling but confers significant accumulation of p53. Wild-type p53 is rapidly degreaded by MDM2, thus there is variability in the western blot ability to pick up the wild-type p53 band (in the 1.1/3.1 mcherry and +WT), as seen in panel D versus A-C.

# Supplemental Figure 3.

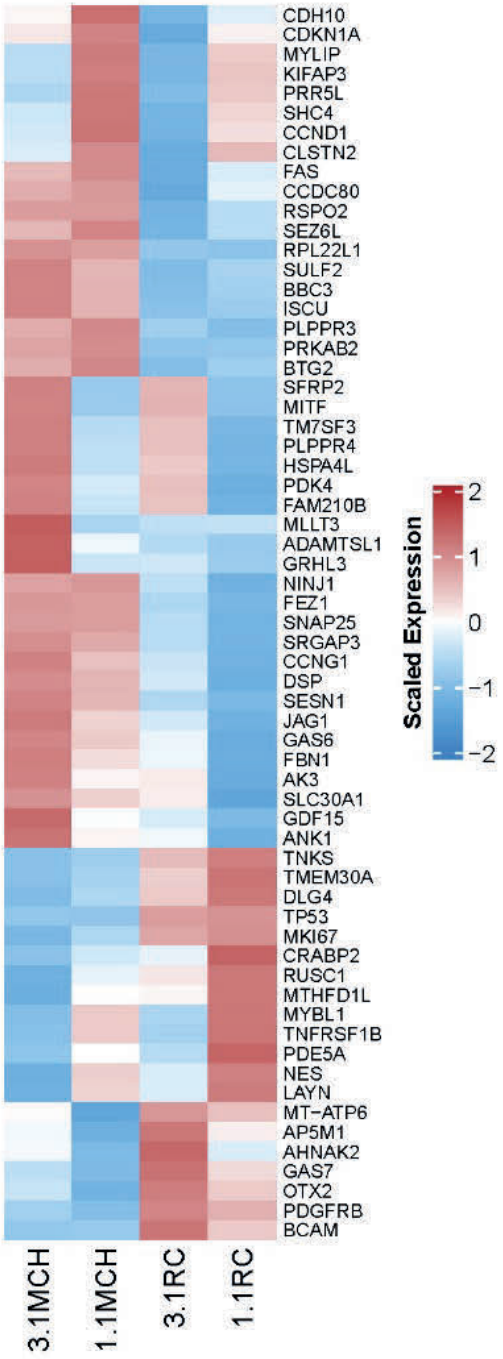


Heat-map of differential gene expression. In this experiment, two NTC (1.1 and 3.1) monoclonal isolates were transfected with mcherry and an R273C allele. Radiation was administered (2Gy) and RNA extracted 24 hours later. Differential gene expression between the lines with only wild-type alleles and those with wild-type + R273C can be appreciated. Notably TP53 expression is confirmed in our 1.1RC and 3.1RC constructs, confirming increased expression via our PGK promoter.

# Supplemental Figure 4.

A

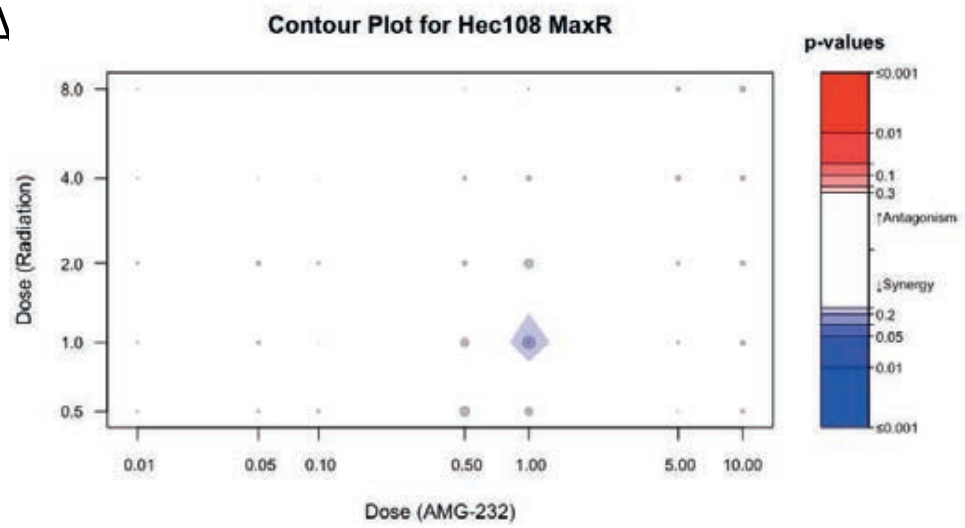


B.

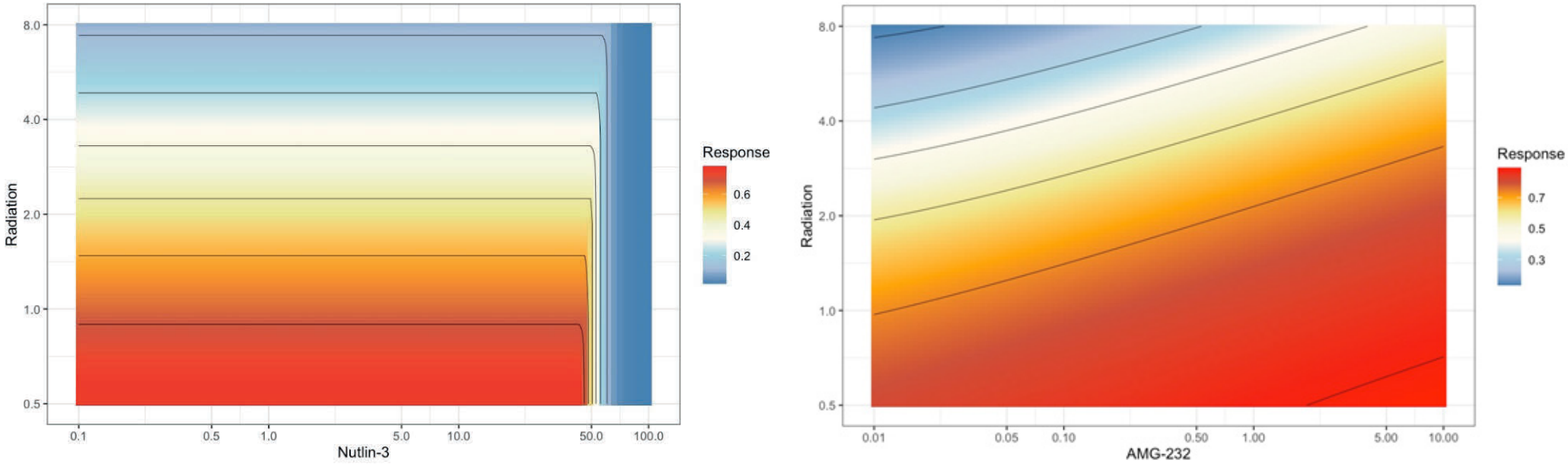


A) Contour plot of HEC108 and AMG-232 demonstrating weak synergy at 1nM and 1Gy dosing. **B)** Isobologram of Hec1B using radiation (y-axis) and drug concentration (x-axis). As noted there is no effect with the addition of Nutlin-3 to radiotherapy and a suggestion of an antagonistic effect at higher doses with AMG-232.

# Supplemental Figure 5.

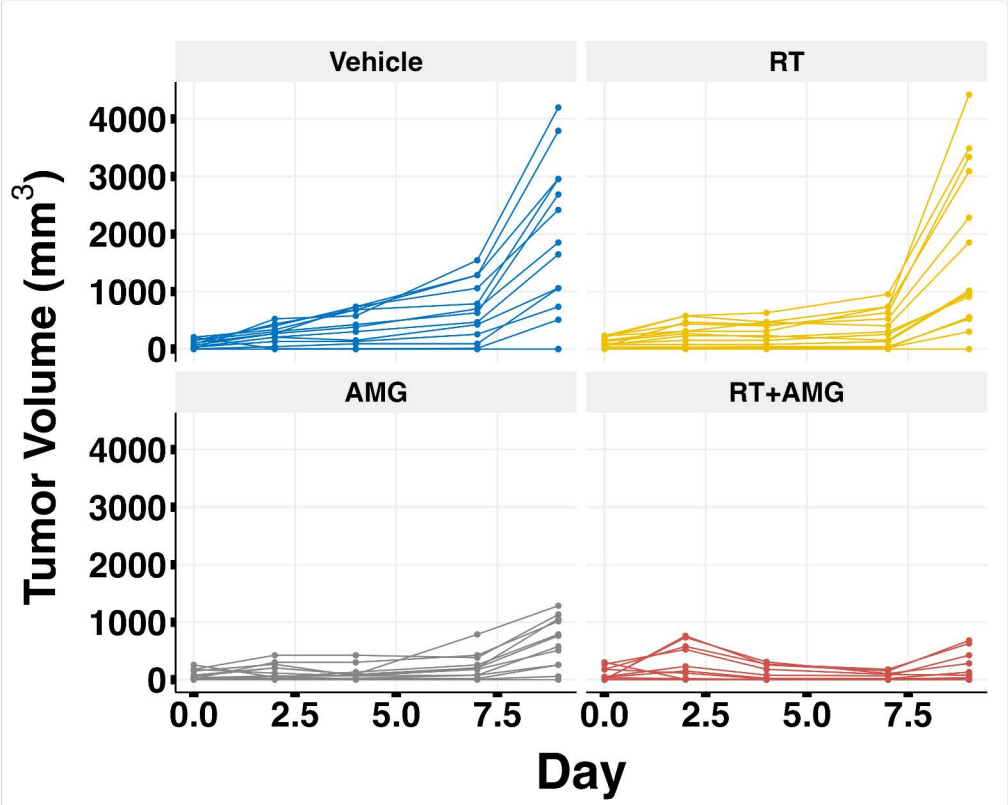


Individual xenograft tumor growth curves based on treatment group. Each line represents an individual tumor through the entire experiment. Each mouse had 2 tumors, one on each flank. We can observe that AMG-232 (bottom left) had a substantial impact on tumor size, while co-treatment with 1Gy of radiotherapy almost eliminated the tumors by day 7 post-treatment.

# Supplemental Figure 6.

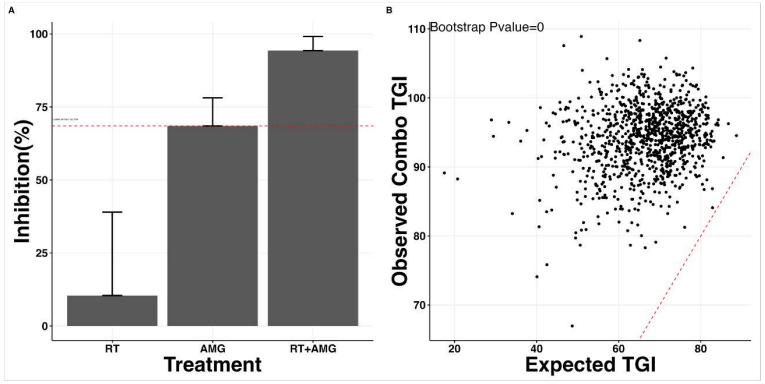


HSA

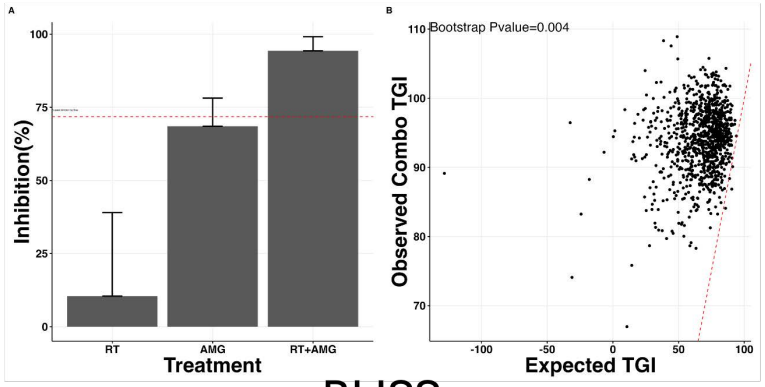


BLISS

*In Vivo* Highest Single Agent (top) and BLISS (bottom) synergy analyses for AMG-232 and Radiotherapy. As seen on the bar graphs (left) tumor growth inhibition (TGI) exceeded an additive effect under both models. Bootstrap analyses using both models (right) confirmed statistically significant synergy compared to expected TGI, as denoted by the dashed line.

# Supplemental Table 1.

| Term | Overlap | P-value | Adjusted P-value | Odds Ratio | Combined Score | Genes |
|---|---|---|---|---|---|---|
| **p53 Pathway** | **9/200** | **3.59E-06** | **1.26E-04** | **8.283096** | **103.8415782** | **CDKN1A;BTG2;SESN1;NINJ1;CCNG1;FAS;TM7SF3;TP53;BLCAP** |
| **Apoptosis** | **6/161** | **4.44E-04** | **0.007778** | **6.639215** | **51.24539677** | **CDKN1A;BTG2;CCND1;GADD45B;PLPPR4;FAS** |
| **TNF-alpha Signaling via NF-kB** | **6/200** | **0.001375** | **0.016047** | **5.294039** | **34.88214092** | **CDKN1A;BTG2;CCND1;GADD45B;NINJ1;IER2** |
| Mitotic Spindle | 3/199 | 0.119967 | 0.422972 | 2.553139 | 5.414022257 | RICTOR;KIFAP3;KIF15 |
| Hypoxia | 3/200 | 0.121286 | 0.422972 | 2.54005 | 5.358499671 | CDKN1A;HOXB9;CCNG2 |
| G2-M Checkpoint | 3/200 | 0.121286 | 0.422972 | 2.54005 | 5.358499671 | CCND1;MKI67;KIF15 |
| Estrogen Response Early | 3/200 | 0.121286 | 0.422972 | 2.54005 | 5.358499671 | SOX3;CCND1;MYBL1 |
| Myogenesis | 3/200 | 0.121286 | 0.422972 | 2.54005 | 5.358499671 | CDKN1A;GADD45B;SCHIP1 |
| mTORC1 Signaling | 3/200 | 0.121286 | 0.422972 | 2.54005 | 5.358499671 | CDKN1A;BTG2;CCNG1 |
| E2F Targets | 3/200 | 0.121286 | 0.422972 | 2.54005 | 5.358499671 | CDKN1A;MKI67;TP53 |

Hallmark pathway analyses using differential gene expression data 24 hours after radiotherapy exposure.

# Supplemental Table 2.

| Target | Target Sequence | F oligo (BsmBI site in red) | R oligo (BsmBI site in red) |
|---|---|---|---|
| NTC 1.1 | GTATTACTGATATTGGTGGG | CACCGGTATTACTGATATTGGTGGG | AAACCCCACCAATATCAGTAATACC |
| NTC 3.1 | TCAACCCCAGCGCACCGTTG | CACCGTCAACCCCAGCGCACCGTTG | AAACCAACGGTGCGCTGGGGTTGAC |
| TP53 5.1 | TGAGGGCAGGGGAGTACTGT | CACCGTGAGGGCAGGGGAGTACTGT | AAACACAGTACTCCCCTGCCCTCAC |
| TP53 6.1 | GTTGCAAACCAGACCTCAGG | CACCGGTTGCAAACCAGACCTCAGG | AAACCCTGAGGTCTGGTTTGCAACC |

CRISPR/Cas9 guide-RNA sequences. A designed 5.1 targets exon 5 and 6.1 targets exon 6.

# Supplemental Table 3.

| Name/mutation | F primer (mutated site underlined) | R primer (mutated site underlined) |
|---|---|---|
| attL flanking sites | (L1) CGTTGTAAAACGACGGCCAGTC | (L2) GCCAGGAAACAGCTATGACCATG |
| TP53 R273H | AGCTTTGAGGTGCATGTTTGTGCCTGT | ACAGGCACAAACATGCACCTCAAAGCT |
| TP53 R273C | AGCTTTGAGGTGTGTGTTTGTGCCTGT | ACAGGCACAAACACACACCTCAAAGCT |
| TP53 R248Q | GGCGGCATGAACCAGAGGCCCATCCTC | GAGGATGGGCCTCTGGTTCATGCCGCC |
| TP53 R248W | GGCGGCATGAACTGGAGGCCCATCCTC | GAGGATGGGCCTCCAGTTCATGCCGCC |
| TP53 Y220C | GTGGTGGTGCCCTGTGAGCCGCCTGAG | CTCAGGCGGCTCACAGGGCACCACCAC |

*TP53* variant site-directed mutagenesis primer sequences with nucleotide substitutions.

Figure 1 - Panel **C** (JHUEM**1**)

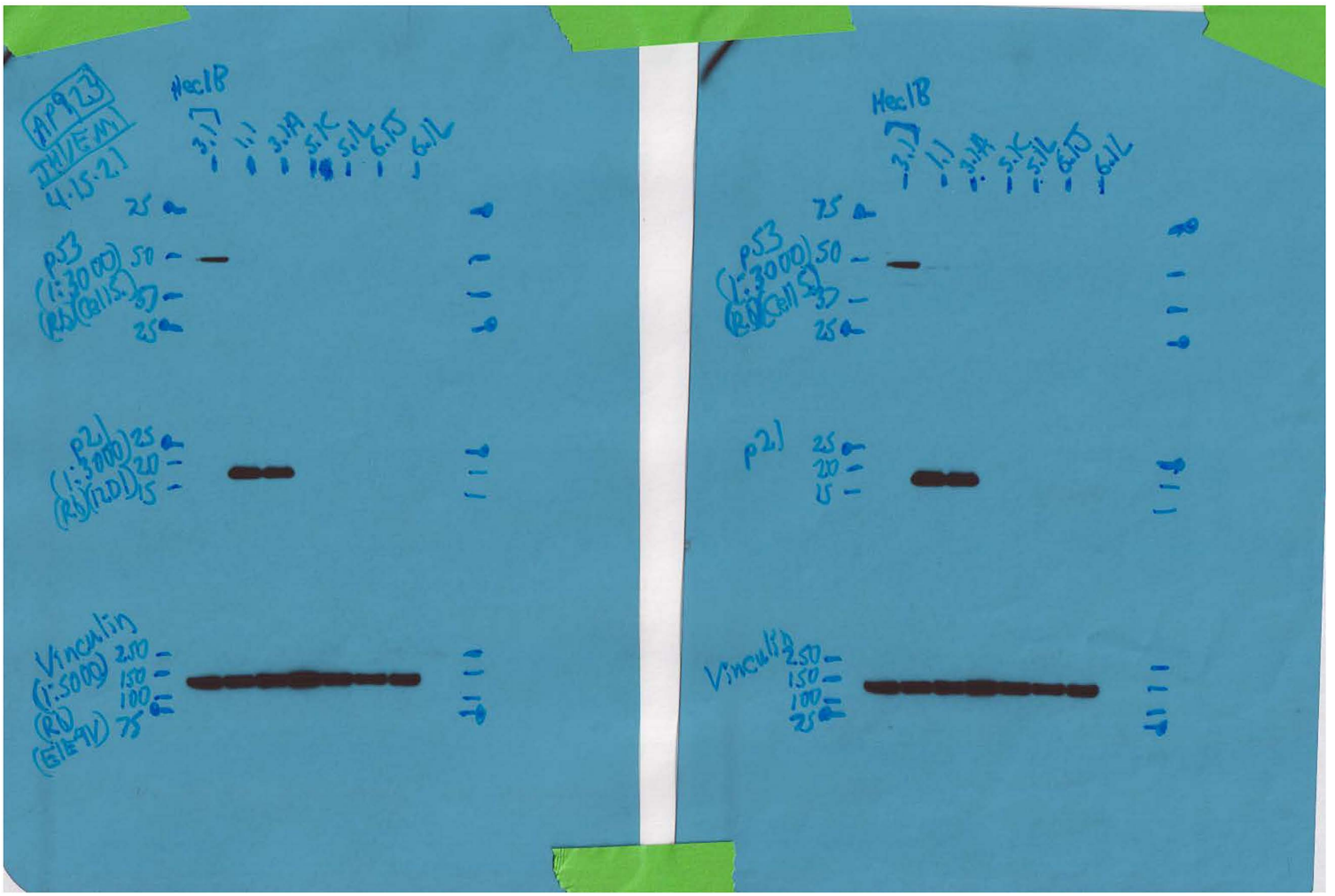


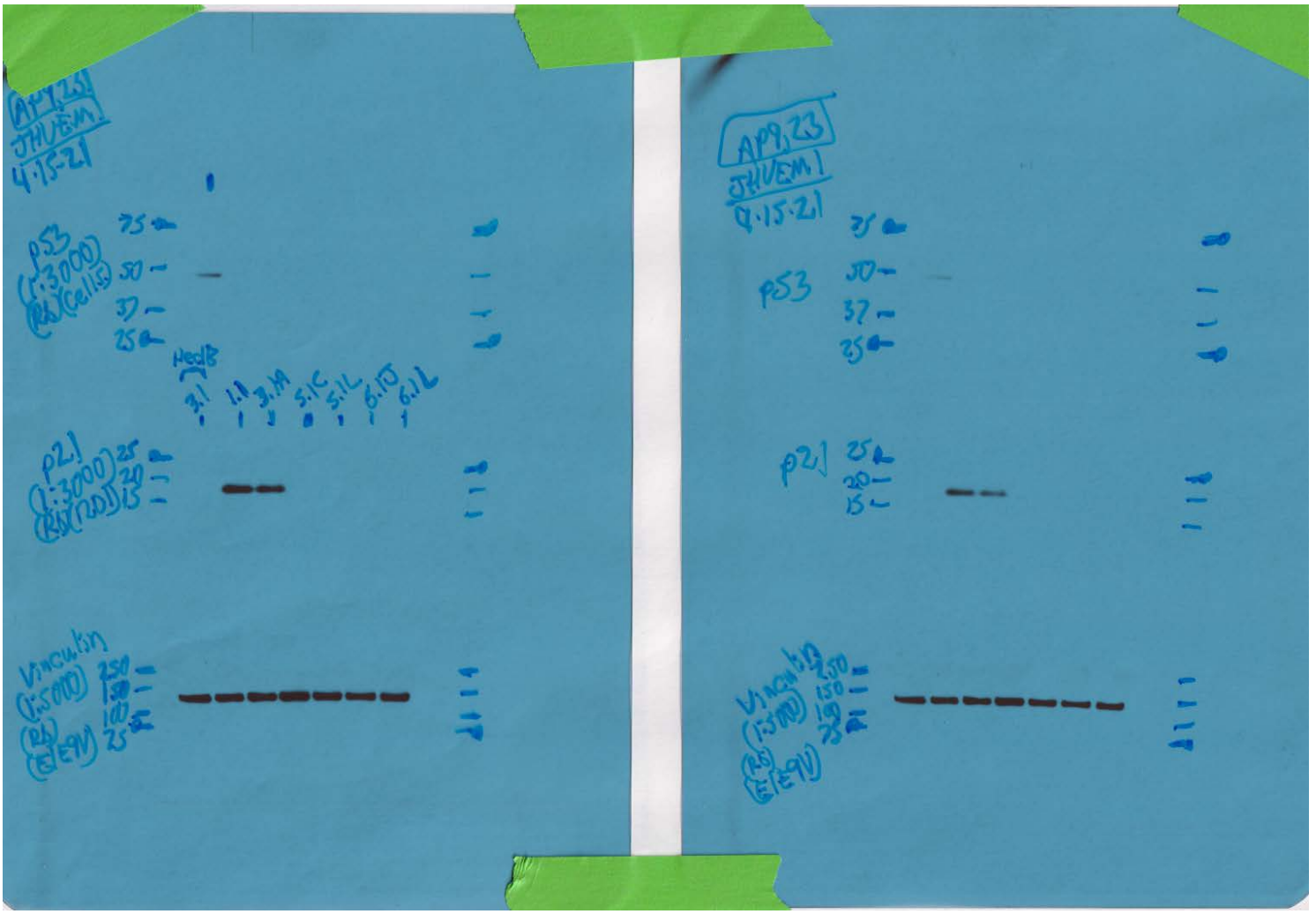

Figure 1 - Panel **C** (JHUEM**2**)

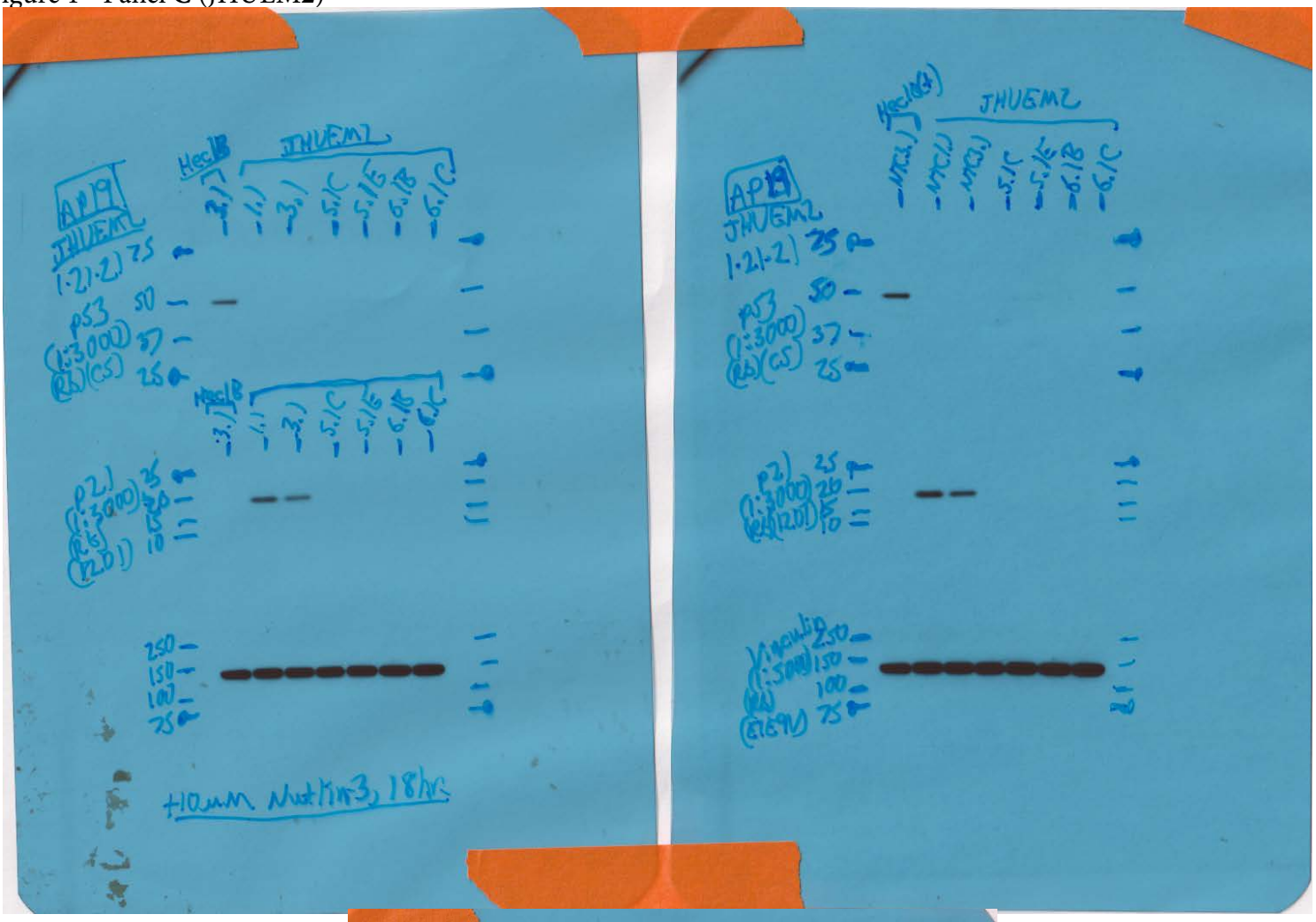


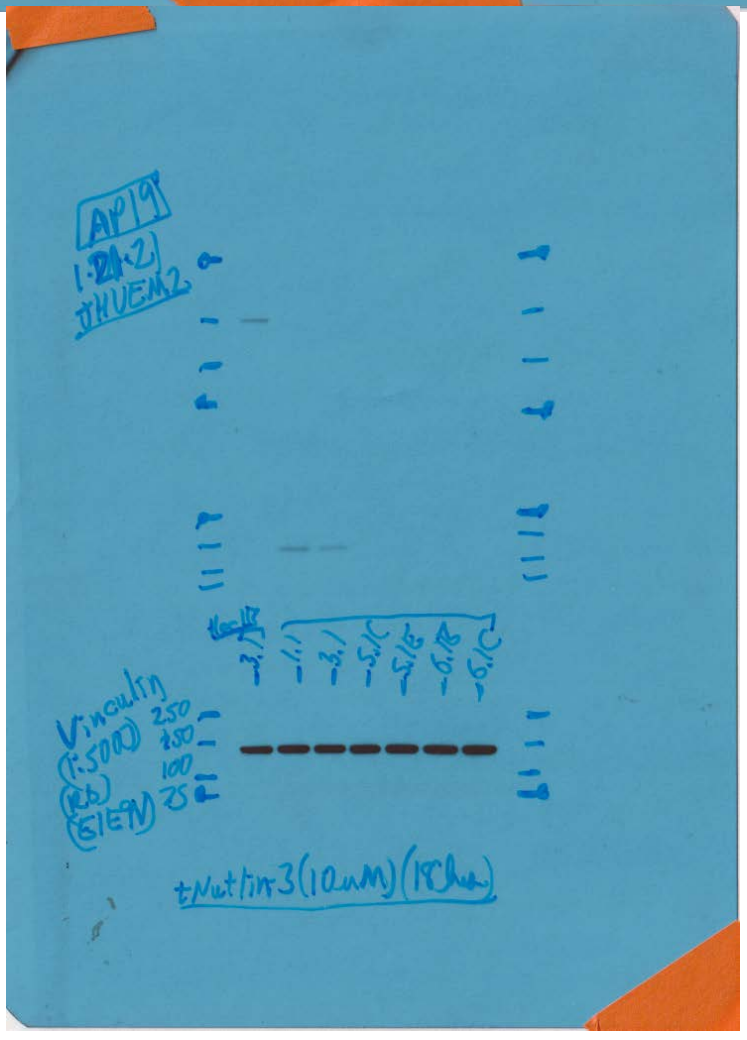

Figure 1 - Panel **D** (JHUEM2 - **5.1** TP53 KO  Addback)

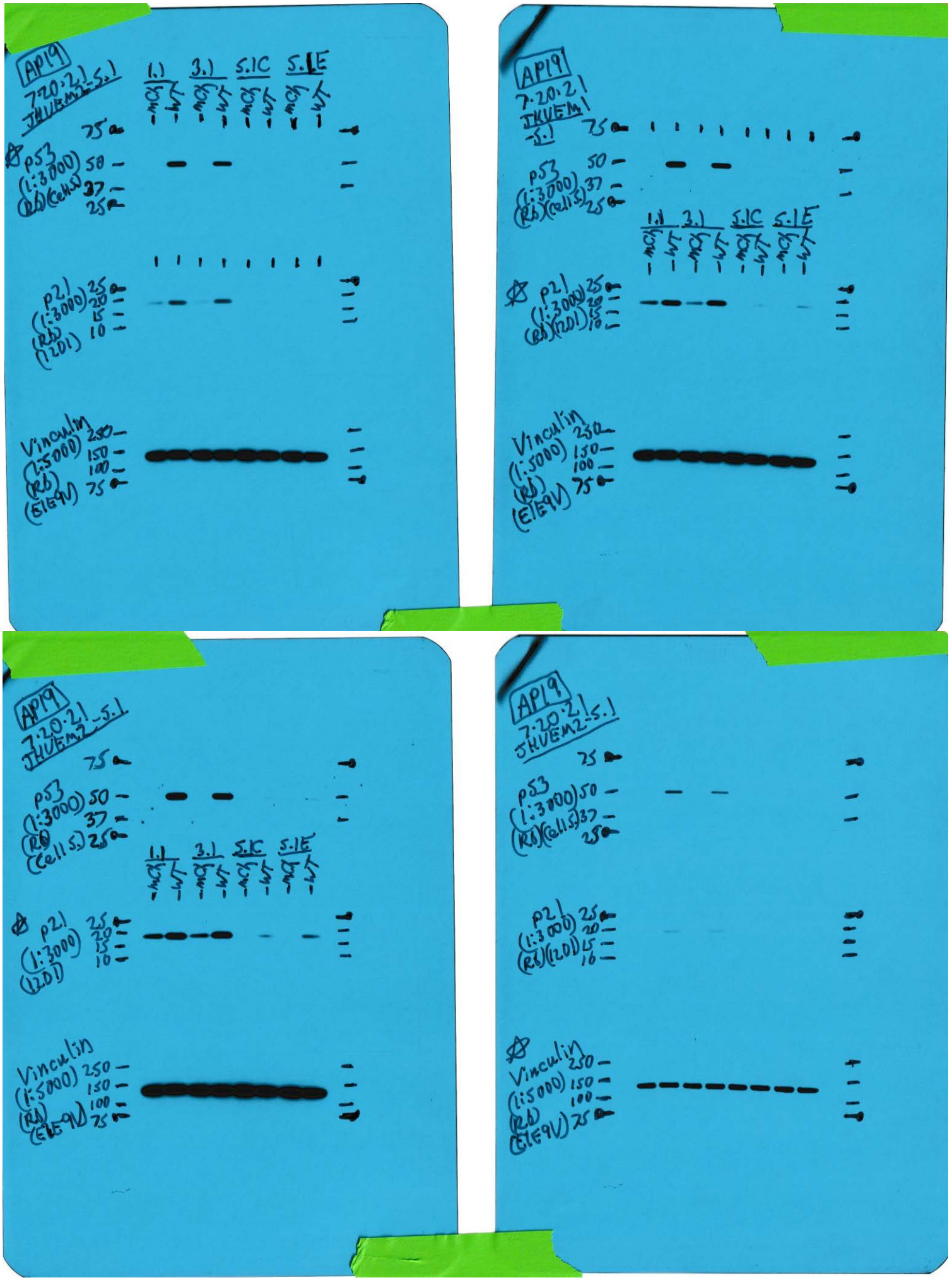

Figure 1 - Panel **D** (JHUEM2 - **6.1** TP53 KO Addback)

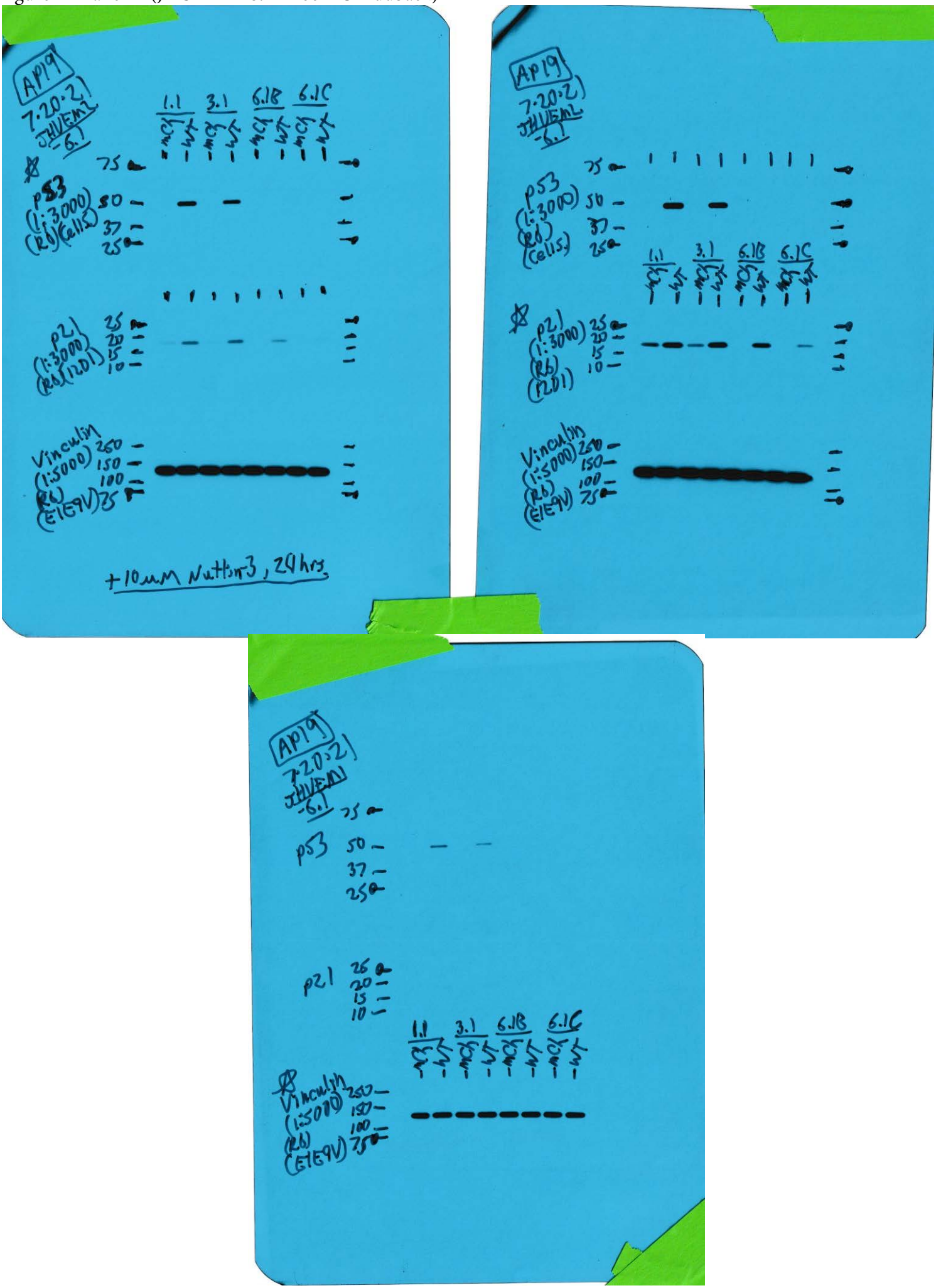

Figure 2 - Panel **A** (JHUEM2 + R273C Variant Dominant-Negative)

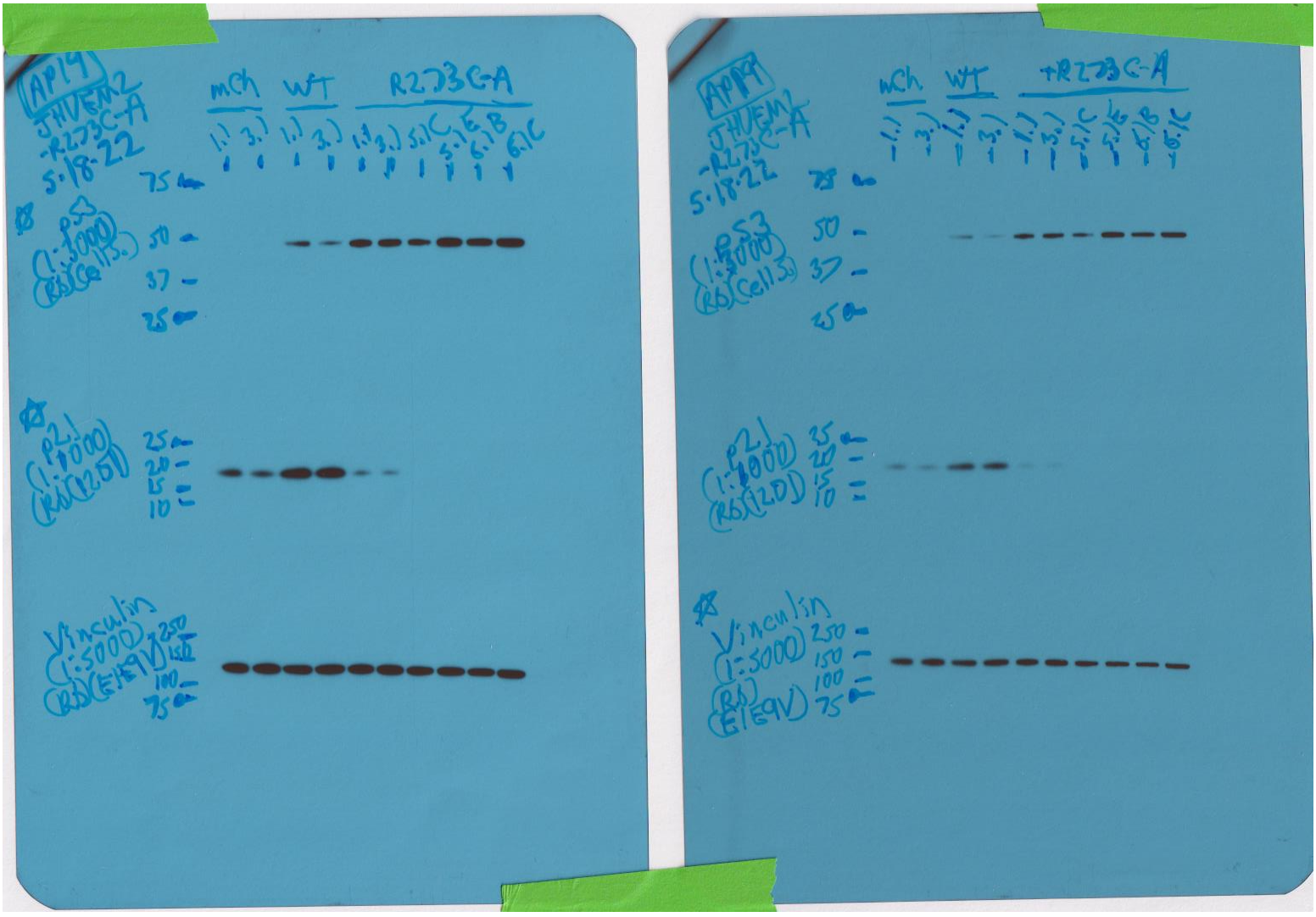

Figure 2 - Panel **C** (JHUEM2 + All TP53 Variants Dominant-Negative)

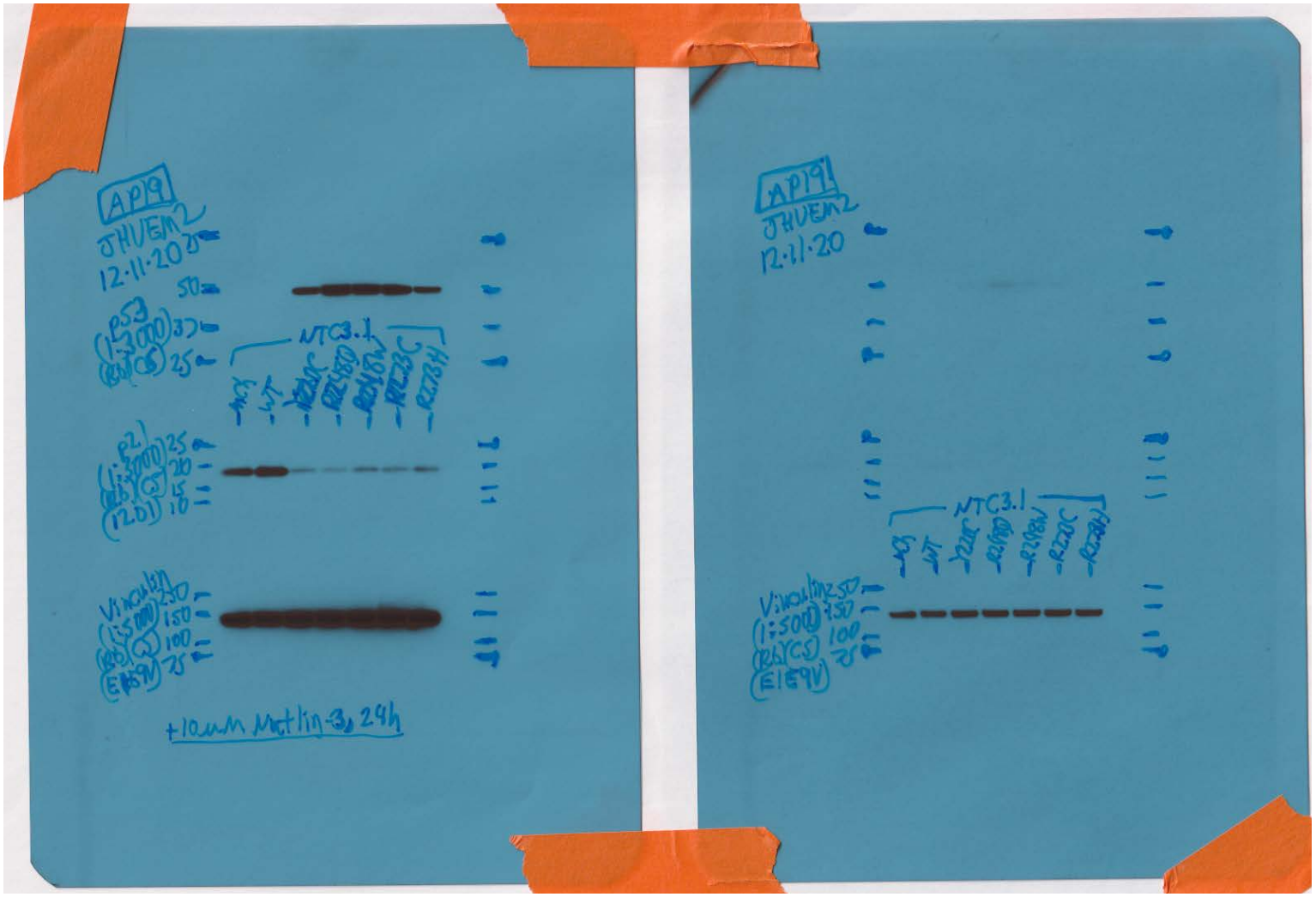


Figure **3** Panel **B** - (Nutlin-3 Response JHUEM2/Hec108/Hec1B)

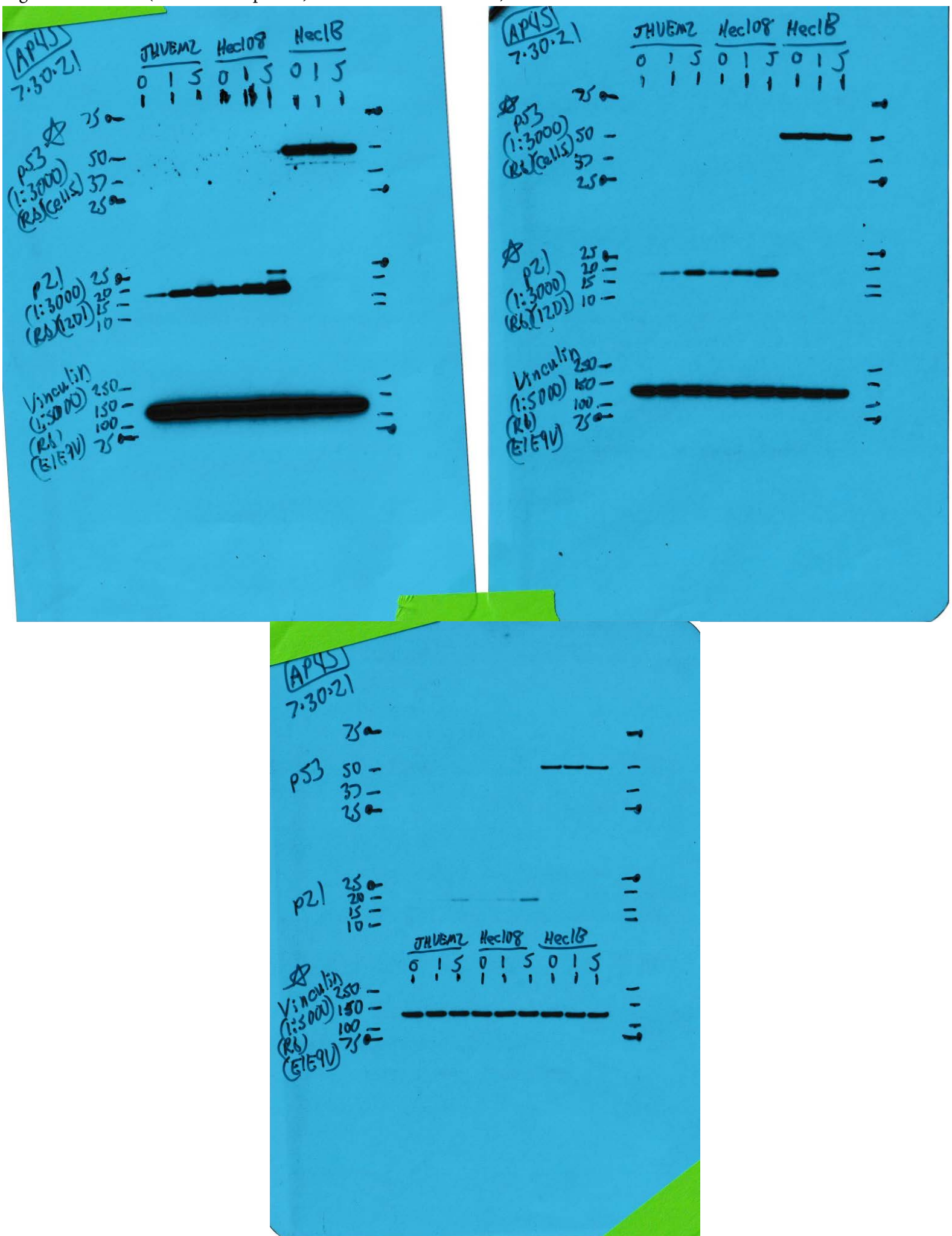

Figure **3** Panel **B**- (Nutlin-3 Response JHUEM2/Hec108 SubFigure)

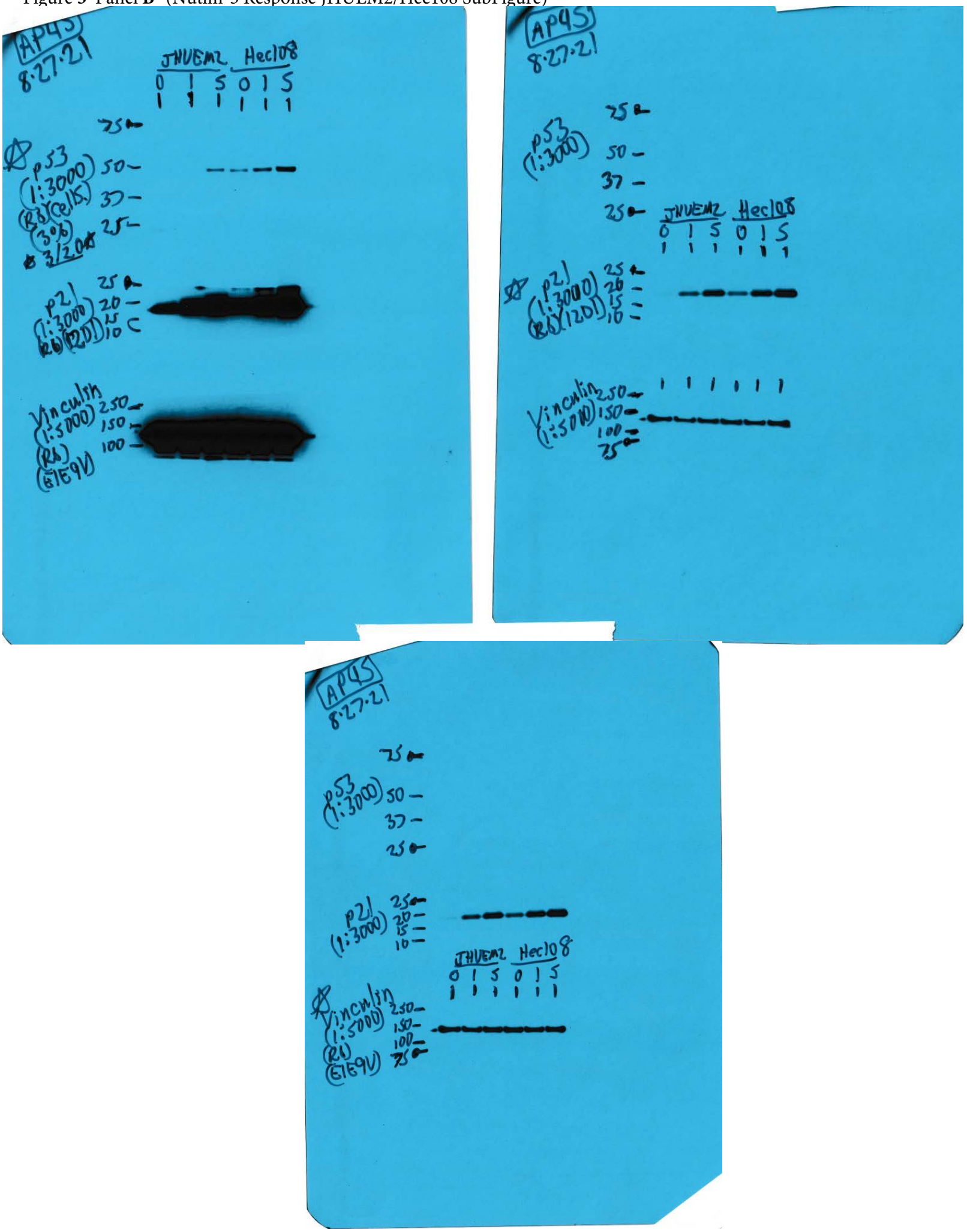

Figure **3** Panel **D**- (AMG-232 Response JHUEM2/Hec108/Hec1B)

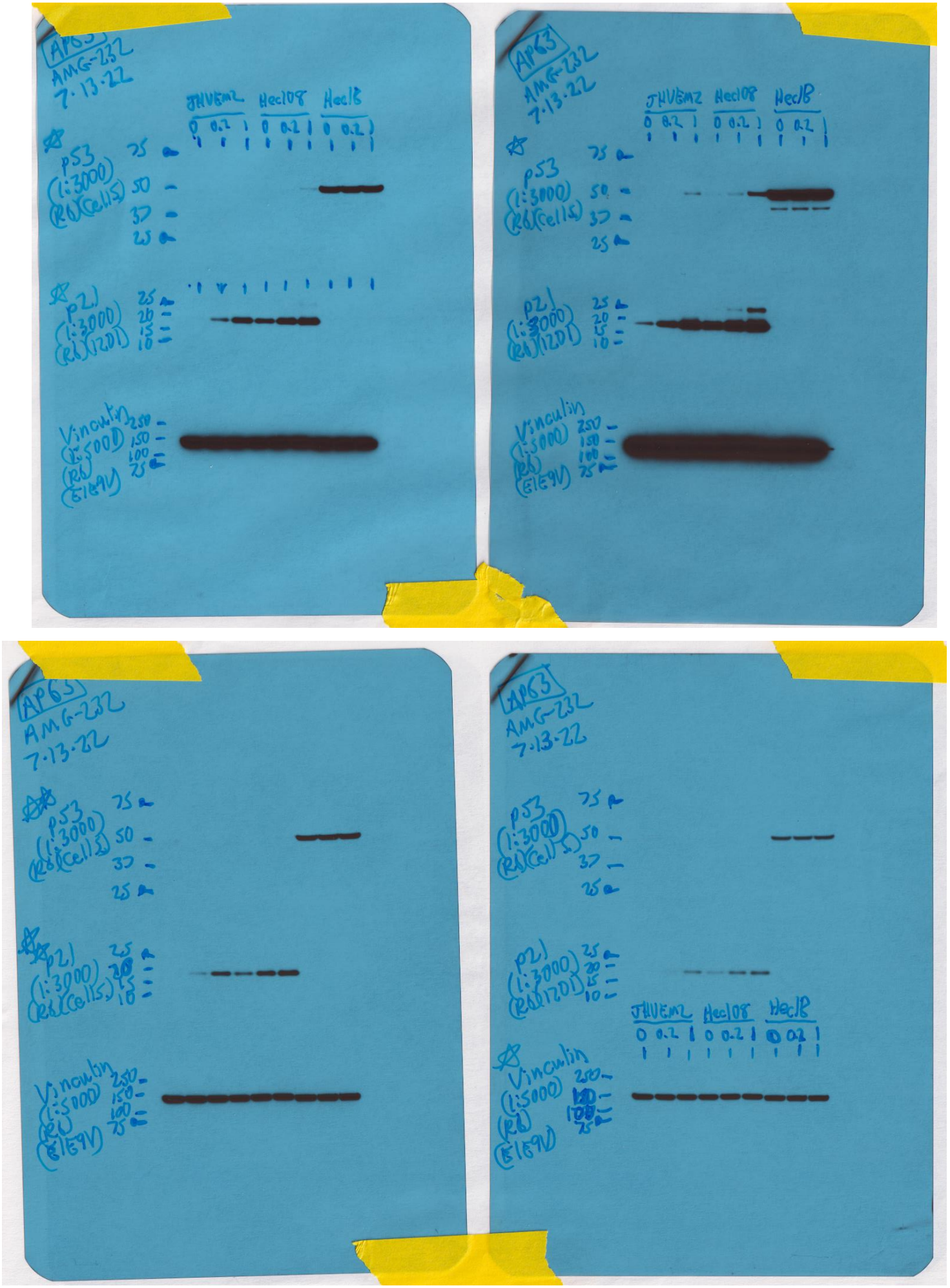

Supplementary Figure 2 - **Y220C**

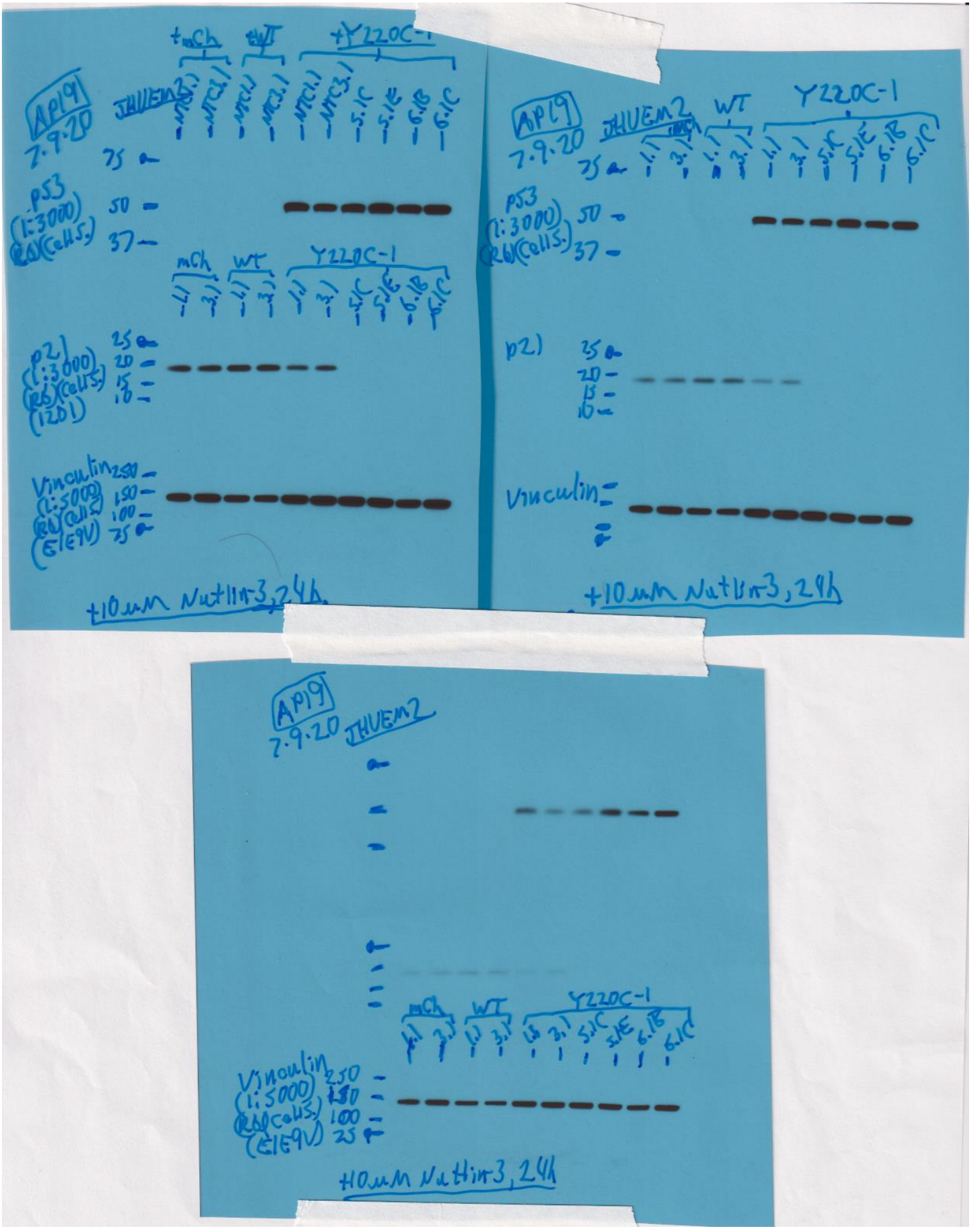

Supplementary Figure 2 - R248Q

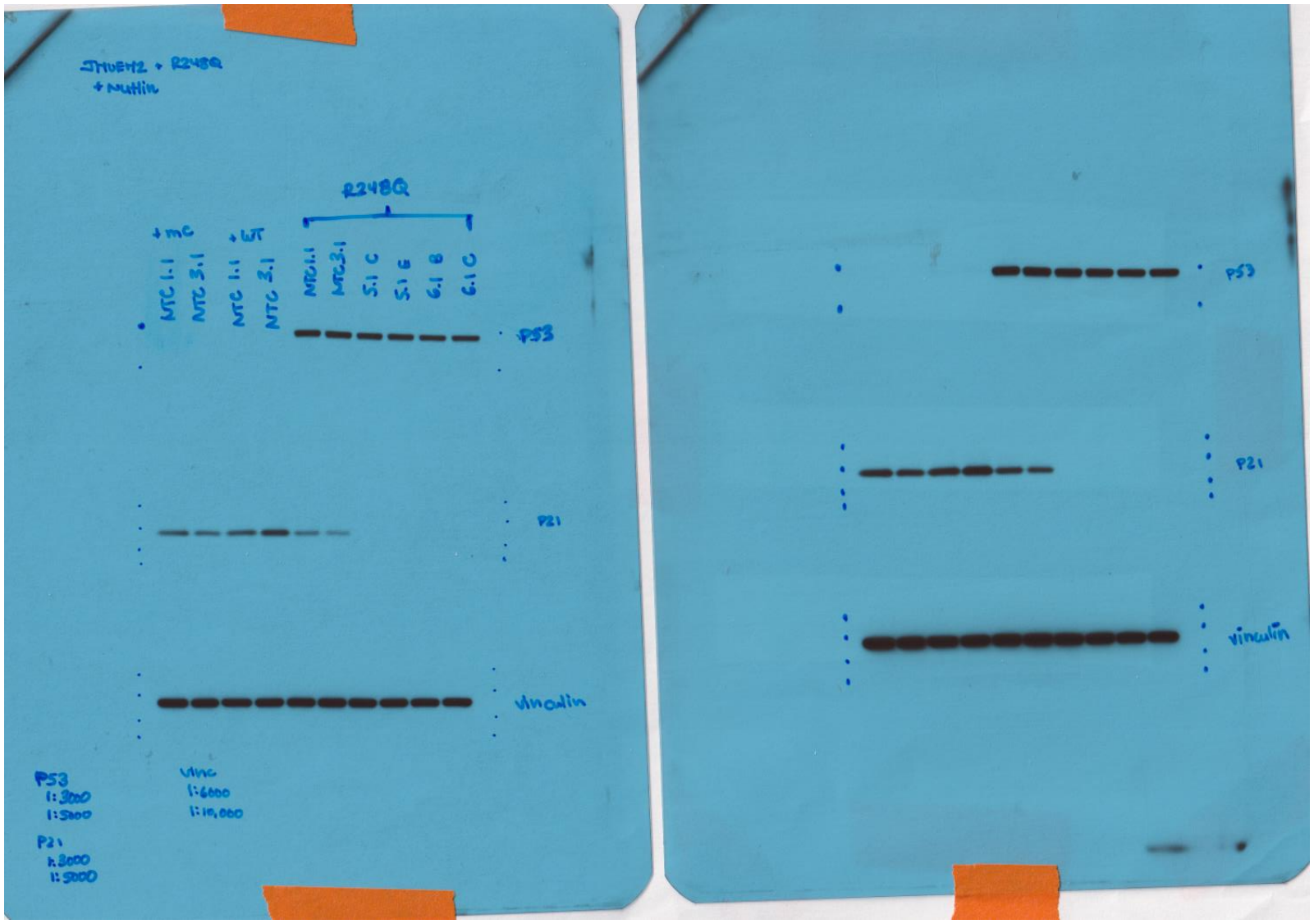

Supplementary Figure 2 - R248W

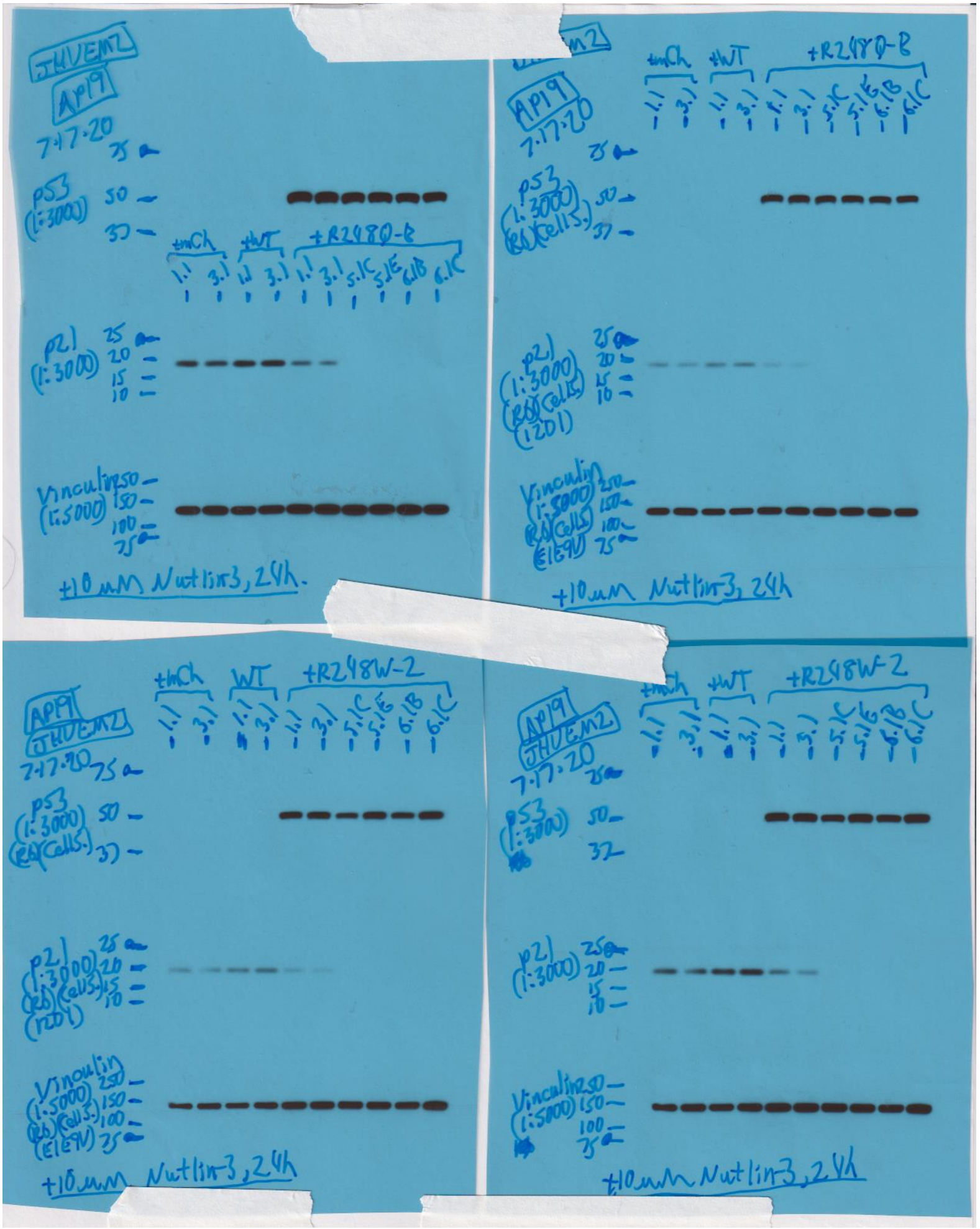

Supplementary Figure 2 - R273H